COMPUTATIONAL FLUID DYNAMICS MODELLING FOR DISPERSION OF ^{14}C RELEASED FROM STACK AND COMPARISON WITH EXPERIMENTAL RESULTS IN THE VICINITY OF PHWR POWER PLANT

Synopsis of the Thesis to be Submitted to the Mangalore University for the Award of the Degree of Doctor of Philosophy in Physics

Submitted by

Bharath

Under the Supervision of

Dr. Karunakara N.

Professor and Coordinator, Medical Physics division

Centre for Advanced Research in Environmental Radioactivity (CARER)

Mangalore University

Mangalagangothri- 574199

September 2023

SYNOPSIS OF THE DOCTORAL THESIS

Date:30.09.2024

Name of the student	Bharath Research Student Centre for Advanced Research in Environmental Radioactivity (CARER) Mangalore University Mangalagangothri - 574199
Name of the Research Guide	Dr. Karunakara N. Professor Centre for Advanced Research in Environmental Radioactivity (CARER) Mangalore University Mangalagangothri - 574199
Title of Ph.D. thesis	Computational fluid dynamics modelling for dispersion of ^{14}C released from stack and comparison with experimental results in the vicinity of PHWR power plant
Work Place	Centre for Advanced Research in Environmental Radioactivity (CARER) Mangalore University Mangalagangothri - 574199
Date of Registration	03.04.2018
Ph.D. Registration No.	MU/EXB/Ph.D./CR.108/Phy./2019-20/E.13 Dated 04.05.2020
Nature of Registration	Full time
Subject	Physics
Faculty	Science and Technology

COMPUTATIONAL FLUID DYNAMICS MODELLING FOR DISPERSION OF ^{14}C RELEASED FROM STACK AND COMPARISON WITH EXPERIMENTAL RESULTS IN THE VICINITY OF PHWR POWER PLANT

1. Introduction:

Carbon-14 (^{14}C) is a pure beta emitter ($T_{1/2}$ = 5730 ± 40 y, E_{max} = 156.5 keV) and occurs naturally in the environment due to cosmic ray induced production in the atmosphere (Libby 1945; Godwin 1962; Stenström et al., 2000; KrajcarBronić et al., 2020). The inventory of naturally produced ^{14}C in the Earth's atmosphere is ~220 × 10^{15} Bq (KrajcarBronić et al., 2020; UNSCEAR, 2010, 2017). The long-term mean value of specific activity of natural atmospheric carbon has been determined to be 226.0 ± 1.1 Bq of ^{14}C per kg of carbon (Bq kg^{-1} C) in the air-borne CO_2 which is equal to 100 pMC (percent of modern carbon) with the year 1950 as the reference date (Karlen et al., 1964; Libby 1965; Stenström et al., 2000; Roussel-Debet et al., 2006). The $^{14}CO_2$ present in the atmosphere gets assimilated by plants through the photosynthesis process, and it is the major pathway of entry of radiocarbon into plants and subsequently to the human being. The ^{14}C specific activity in terrestrial plants is expected to be in equilibrium with that of in atmosphere and equilibrium is achieved relatively quickly. The annual effective dose to the public due to naturally produced ^{14}C in the environment is ~12 μSv (UNSCEAR 1977).

Atmospheric nuclear tests, during the 1950s and 1960s, increased the specific activity in the environment significantly (termed as "Bomb Effect"), reflected in a maximum of atmospheric ^{14}C activity in 1963 of about twice the natural in the northern hemisphere (Levin et al., 1985). The estimated release of ^{14}C into the atmosphere by weapon tests is ~2.2 × 10^{17} Bq (UNSCEAR, 1993, 2000). ^{14}C is also released into the

atmosphere by nuclear fuel cycle facilities and gaseous discharges from all types of nuclear power plants (NPPs). In nuclear reactors, ^{14}C is produced by the neutron activation of stable isotopes of carbon, nitrogen and oxygen in the fuel, cladding, coolant, moderator, and structural materials of the reactor (IAEA 2004a; Mazeika et al., 2008). Owing to the presence of a large mass of D_2O as a moderator and higher neutron flux, the extent of ^{14}C produced through the neutron activation of ^{17}O in a CANDU type reactor is greater than any other reactor type (Sohn et al., 2004). According to UNSCEAR (2000), the average-normalized release rates of ^{14}C from different types of nuclear power reactors are 1.6, 1.3, 0.51, and 0.22 TBq $GW(e)^{-1}a^{-1}$, respectively for Canada Deuterium Uranium (CANDU), Reaktor Bolshoy Moshchnosti Kanalniy (RBMK), Boiling Water Reactor (BWR), and Pressurized Water Reactor (PWR) types of reactors. The ^{14}C releases occur mainly in two chemical forms; oxidized, i.e. carbon dioxide (CO_2), and reduced, mostly in CH_4 (Joshi et al., 1987; Zazzeri et al., 2018). The oxide form is the dominant form of the ^{14}C release through gaseous effluents in all types of nuclear reactors, except PWRs (IAEA, 2004). The gaseous release of ^{14}C in the form of $^{14}CO_2$ is assimilated by plants (IAEA 2004a). As a consequence, the increased specific activity of ^{14}C may be found in biota in the vicinity of NPPs. Considering the biological importance of ^{14}C in the organism and its long half-life, significant importance is given to monitoring its activity in the region around the NPPs (Stenström et al., 2011).

Long-term monitoring of ^{14}C around French NPP sites (Roussel-Debet et al., 2006), around Cernavoda NPP, Romania (Popoaca et al., 2014) and Bohunice NPP, Slovakia and Dukovany NPP, Czech Republic (Povinec et al., 2015) have shown that the dose to the public due to gaseous release was up to 3 μSv y^{-1}. Since the ^{14}C release rate from

the HWR type of reactors is higher when compared to that from the LWRs, the excess activity in the environment in the vicinity of the former is expected to be higher.

Computational Fluid Dynamics (CFD) is a simulation tool used to quantitatively predict the transport of gaseous and liquid phases in a medium under complicated situations. Problems in flow and diffusion-related phenomena described by partial differential equations are often difficult to solve analytically. In such situations, CFD based simulation models are widely used. CFD code solves the relevant science-based mathematical equation, using information about the circumstances in question. It is particularly useful in predicting the conditions in situations where it is not possible to take detailed measurements due to various constraints, such as high temperature, non-accessibility, or dangerous environment etc. It is a diagnostic computer model for simulating atmospheric processes related to pollution hazards.

Dispersion modelling using CFD is a relatively recent development and has been tried for complex terrains, topography, presence of obstacles, etc. (Hsiesh et al., 2013; Mazzoldi et al., 2008, 2011; Hill et al., 2011: Xing et. al., 2013). For dispersion modelling over complex terrains and different meteorological conditions, CFD models are more appropriate. Stenström et al. (1996) have suggested that to test dispersion models, however, air sampling both at the source of the emission and in the surrounding regions are more preferred. Mazzoldi et al. (2011) have reported a comparative study on the application of CFD and other models for simulation of ^{14}C dispersion in the environment. Dispersion models have advantages in emergency preparedness programs for quantification of the pollutants transportation in the atmosphere and to identify the factors affecting its transportation in the environment.

2. Importance of the study

India has a programme to increase nuclear energy production by constructing new power plants to meet the increasing energy demand of its growing population. In this context, it is important to ensure that the environment impact in the process of increased energy production is kept as low as possible. Quantification of gaseous release rate of radioactivity from the NPP is essential for environmental impact and dose assessments. But, a comprehensive study aimed at monitoring the oxide and reduced forms of ^{14}C release through gases effluents and the excess activity in the vicinity of an NPP in India has not been reported so far from other researchers of India, except a few publication from CARER, Mangalore University (Bharath et al., 2021, Bharath et al., 2022). This study was taken up with an objective of standardizing the methods for sampling and the measurement of ^{14}C concentration in the atmospheric air and gaseous effluents from the NPP.

Modelling studies are becoming increasingly important for predicting the fate of pollutants in the environment. The computer codes, such as CFD are extensively used for the prediction of the source, dispersion and sink for the pollutant in the environment. It allows for performing 3-D analysis and to predict the wind flow, velocity, temperature and concentration of the fields. CFD models with high-speed computing systems play a crucial role in emergency situation in nuclear power plants since they can quickly predict the direction of plume progression, dispersion and critical region in the public domain for taking immediate counter measures. While CFD models have been successfully tested for such applications in developed countries for flat terrains, their applications for a complex environment such as Kaiga are yet to be validated. Therefore, the second objective of this study was to evaluate the application of the CFD model to simulate the dispersion of ^{14}C released from the stack from the nuclear power

station for different meteorological conditions in complex terrains, such as Kaiga region, and validate the results through actual measurements of ^{14}C activity in the atmospheric air at different ground monitoring points.

3. Aim and objectives

The aims and objectives of the studies are:

- To standardize a method for sample collection and measurement of ^{14}C in the atmospheric air and gaseous effluents from the NPP.
- To quantify the oxide and reduced form of ^{14}C release rates through gaseous effluents from Kaiga PHWR NPP.
- To quantify excess ^{14}C in atmospheric air in the vicinity of the Kaiga NPP.
- Evaluate the applicability of CFD modelling to predict the dispersion of ^{14}C released from the stack of the NPP under different wind regims and meteorological conditions in a complex terrain such as Kaiga region.
- Validation of the CFD predicted results through actual measurements of ^{14}C activity concentration in atmospheric air.

4. Overview of the work done

4.1 Study area

Kaiga NPP (14º51′51.96″N, 74º26′21.84″E) is situated at an aerial distance of ~ 32 km from the West Coast town of Karwar, India. Four pressurized heavy water reactors (PHWRs), each of 220 MW(e), are in operation at this site with a cumulative installed power capacity of 880 MW(e) (Karunakara et al., 2000; Karunakara et al., 2001; Karunakara et al., 2013 a&b; D'Souza et al., 2019; Nayak et al., 2019; Kamath et al., 2019). The first two reactors (Kaiga 1 & 2) were commissioned in 2000, and the

third and fourth (Kaiga 3 & 4) reactors were commissioned in 2007 and 2011, respectively. Gaseous effluents of Kaiga 1 & 2 are released through stack-1 and those of Kaiga 3 & 4 through stack-2. The reactors are designed to use natural uranium dioxide as fuel with D_2O as moderator, coolant and reflector. The aerial view of the NPP is given in Fig. 1.

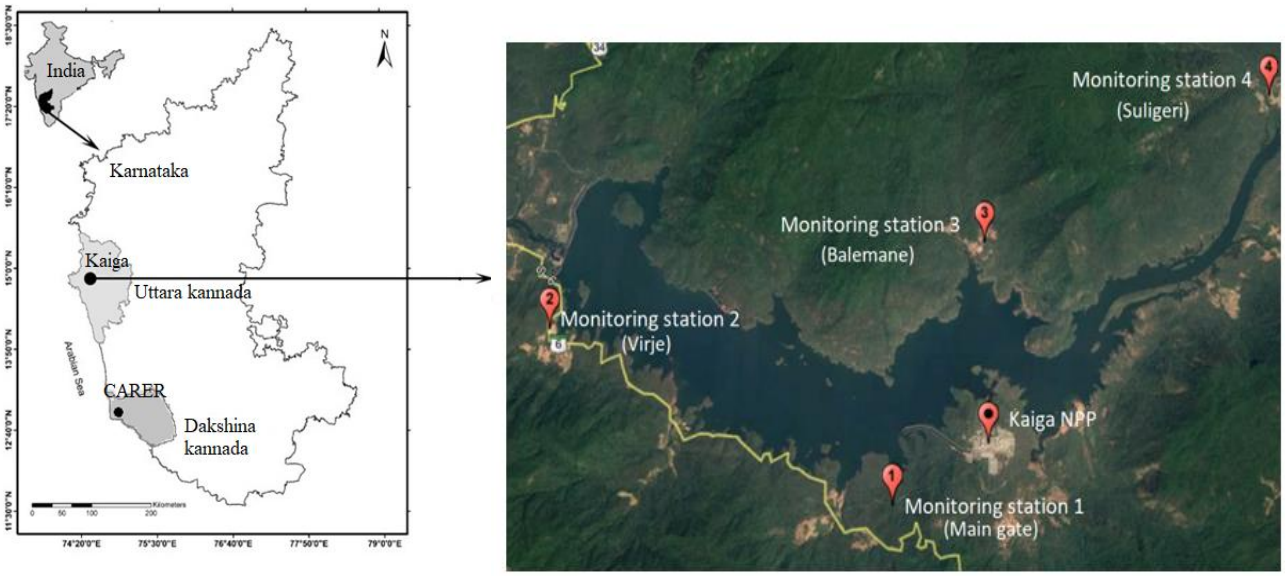

Fig.1.Map showing the location of Kaiga PHWR NPP on West Coast of India (left), and enlarged map of Kaiga region with ambient air sampling station (right)

Kaiga is adjoined to the river Kali and is situated in the valley of the Western Ghats, which is famous for its biodiversity. Several streams flow through the mountains, join the river Kali and finally meet the Arabian Sea at Karwar. A dam has been constructed on this river at Kadra (about 10 km aerial distance on the downstream side of the NPP), which provides requisite freshwater for the cooling of the condenser system of the power plant. Due to hills and dense forests, Kaiga manifests unique meteorological and ecological characteristics typical of Western Ghats. The topography of this NPP site is considered complex due to the presence of hills, ridges, and dense forest along the Kali River and its estuaries (Sharma et al., 2011). The altitude of the hills and ridges around the NPP varies from 40 m to 600 m. The dominant wind

direction is westerly and south-westerly during rainy and summer seasons and easterly during winter but is known to change within a day several times due to strong westerly wind originating from the Arabian Sea. The wind direction is aberrated by the topography of the region. The annual rainfall in the region is ~ 4000 mm y^{-1}, with the bulk of the contribution from the tropical southwest monsoon (during June – October) originating from the Arabian Sea. The climate is humid, and the annual ambient temperature varies from 22 to 35 °C.

4.2 Standardization of method of ^{14}C determination in atmospheric air

4.2.1 Earlier studies on ^{14}C activity measurement in India

As far as the Indian subcontinent is concerned, the first measurement on ^{14}C release through stack effluent was reported by Joshi et al. (1987) for Rajasthan Atomic Power Station (RAPS). In this method, the sample from the gaseous effluent from the stack was drawn through a series of two gas washing bottles with 250 mL 4N NaOH solution at a flow rate of 0.78 L min^{-1} for seven days to collect the CO_2. A setup with a furnace with CuO catalyst and two additional washing bottles with 4N NaOH was used for quantifying the ^{14}C present in the form of oxides and hydrocarbons. Upon completion of sampling, the Na_2CO_3 was precipitated as $BaCO_3$, and about 0.3 - 0.4 g of dried carbonate sample was introduced into the regeneration and absorption assembly. CO_2 was regenerated from the $BaCO_3$ sample by acidification (lactic acid) and reabsorbed in a 10 mL mixture of ethanolamine and methanol (1:4 V/V). The time required to complete the absorption process was ~ 4 h (Joshi et al., 1987). The ethanolamine and methanol mixture was then mixed with a scintillator (toluene based) and taken for LSC. The overall counting efficiency varied between 45 % and 60 %. This method is suitable for the measurement of ^{14}C from stack release because of the high specific activity to be measured.

Recently, the above method was examined for its applicability to determine the ^{14}C specific activity in ambient air in the vicinity of the nuclear facility at Tarapur Atomic Power Station (Baburajan et al., 2020). The procedure and experimental setup adopted by these authors for sampling air, $BaCO_3$ precipitation, CO_2 regeneration and LSC were similar to that reported by Joshi et al. (1987). From the count rate obtained from the LSC analysis of the sample, the ^{14}C activity was calculated as under (Baburajan et al., 2020):

$$A = \frac{(GC - B)}{(60 \times E \times V \times f \times R \times Q)} \pm \frac{\sqrt{(GC + B) \times T}}{(T \times 60 \times E \times V \times f \times R \times Q)} \qquad (1)$$

where,

A is the activity (Bq m^{-3}),

GC is the count rate (cpm) due to sample + background,

B is the background count rate (cpm),

T is the counting time (min),

E is the counting efficiency, (fraction, < 1),

V is the volume of air passed through the bubbler (m^3),

f is the percentage absorption of CO_2 in NaOH depending upon the stages of bubblers used in series for the sampling (< 1),

R is the recovery factor (< 1) of carbon species in the entire analytical process ($BaCO_3$ precipitation, its acid hydrolysis and the absorption of evolved CO_2 in ethanolamine – methanol mixture), and

Q is the portion of $BaCO_3$ taken (from the total precipitate obtained) for CO_2 regeneration (< 1).

From the activity (Bq m^{-3}), the specific activity of ^{14}C (Bq $kg^{-1}C$) was computed by using a generalised value of carbon content in the air (0.2 gC m^{-3}, IAEA, 2010).

4.2.2 Difficulties associated with the above-discussed method

Several difficulties exist with the method discussed above when the ambient air is analysed for ^{14}C activity and hence not suitable for this application. This is because of the minimal mass (~0.8 g) of the $BaCO_3$ taken for CO_2 regeneration and absorption in the absorber, as well as the combined uncertainty introduced due to the approximations for the different factors in the denominator of Eq. 1. The details of these are discussed below.

(i) Uncertainty in the estimation of the volume of air passed through the bubbler (V):

(ii) Uncertainty in the percentage absorption of CO_2 in NaOH in the bubbler setup (f):

(iii) Uncertainty in the analytical recovery (R) of carbon species during $BaCO_3$ precipitation, regeneration and the absorption of evolved CO_2 by ethanolamine–methanol mixture: knowledge on the recovery factor for carbon species in the entire chemical process is essential for the activity calculation (Eq. 1).

(iv) The other significant source of uncertainty is factor Q, the portion of $BaCO_3$ taken for CO_2 regeneration.

(v) Information on the carbon content (gC m^{-3} of air) of the sample is also essential for computing the specific activity (Bq $kg^{-1}C$), and the determination of this necessitates an additional analysis of the samples based on methods such as the use of elemental analyser (Singleton et al., 2002; D'Souza et al., 2019).

(vi) The other parameters affecting the measurement is the correction for the counting efficiency due to quenching exhibited by the CO_2 loaded absorber and the background count rate.

All these contribute to the high uncertainty, low accuracy and precision (with deviations more than 30 % from the target value), and high value for minimum detectable activity (MDA) in the method. For example, the MDA reported by Baburajan et al. (2020) is 250 Bq $kg^{-1}C$ (at 2σ), which is well above ambient ^{14}C specific activity in clean air region and hence rendering this method inapplicable for ambient air ^{14}C specific activity measurements quantifying and small excess activity in the vicinity of a nuclear facility. Another disadvantage of this method is the significantly long time (~ 12 h) required to complete the CO_2 absorption process. The environmental impact assessment studies around the NPP involve the analysis of a large number of samples in a short time, and hence methods that allow the determination of radionuclide activities in the shortest possible processing time is preferred with still reasonably good accuracy and precision.

4.2.3 Improved method - determination of specific activity by saturating the absorber

The difficulties and uncertainties associated with the method discussed above can be overcome by improvement in the method. In the improved method, the absorber is saturated with CO_2 released from the carbonate sample, and the mass of the CO_2 absorbed is determined gravimetrically. Woo et al. (1999 a&b), Noakes et al. (2006), Molnar et al. (2006), Horvatinčić et al. (2004), Qureshi et al. (1989), Krajcar Bronić et al. (2009), Canducci et al. (2013), Varlam et al. (2007), Vagner et al. (2019), Leaney et al. (1994), Nair et al. (1995), Norton and Devlin (2006) and D'Souza et al. (2021) have

employed this method for the quantification of CO_2 loaded on the absorber and have discussed the advantages of this method. From the mass of the CO_2 absorbed and from LSC of the absorber-scintillator mixture, the specific activity was computed as under:

$$A = \frac{C \times 100 \times 44.01}{60 \times E \times W \times 12} \pm SD \qquad (2)$$

where,

A is the specific activity of ^{14}C (Bq $kg^{-1}C$),

C is the net count rate (cpm) from the sample, $C = \frac{(C_S - C_b)}{T}$, C_s is the gross counts, and

C_b is the background counts,

T is the counting time (min),

W is the mass (kg) of the CO_2 absorbed in the absorber,

E is the counting efficiency (%), the factor 44.01 corresponds to the molecular mass of CO_2, and

SD is the standard deviation computed as under (IAEA/RCA, 1989)

$$SD = \left(\sqrt{\frac{C_s}{T^2}} + \sqrt{\frac{C_b}{T^2}} \right) \times \frac{100 \times 44.01}{60 \times E \times W \times 12} \qquad (3)$$

(i) As evident from Eq. 2, the volume of air sampled, the trapping efficiency, and the chemical recovery are not essential parameters for ^{14}C specific activity calculation in this method, and hence the uncertainties associated with the determination of these parameters and hence associated uncertainty in the measured value of specific activity are alleviated.

4.2.4Development of a new CO_2 regeneration and absorption system for saturating the absorber

Efficient handling of ~13 g $BaCO_3$, required for saturating the absorber, calls for the design and development of an improved CO_2 regeneration-absorption setup and this was realised in the present work. The improved CO_2 regeneration set up is shown in Fig. 2 and is similar to the one demonstrated by Woo et al. (1999b). The carbonate sample was taken in the reaction vessel, and 4N HCl was added slowly from the funnel arrangement with constant stirring to liberate CO_2 in a controlled way. N_2 gas was purged to the reaction vessel at a flow rate of ~0.05 L min^{-1} and the CO_2 produced was trapped in 10 mL + 10 mL absorber–scintillator mixture (previously weighed, accuracy of 0.1 mg), through a bubbling process.

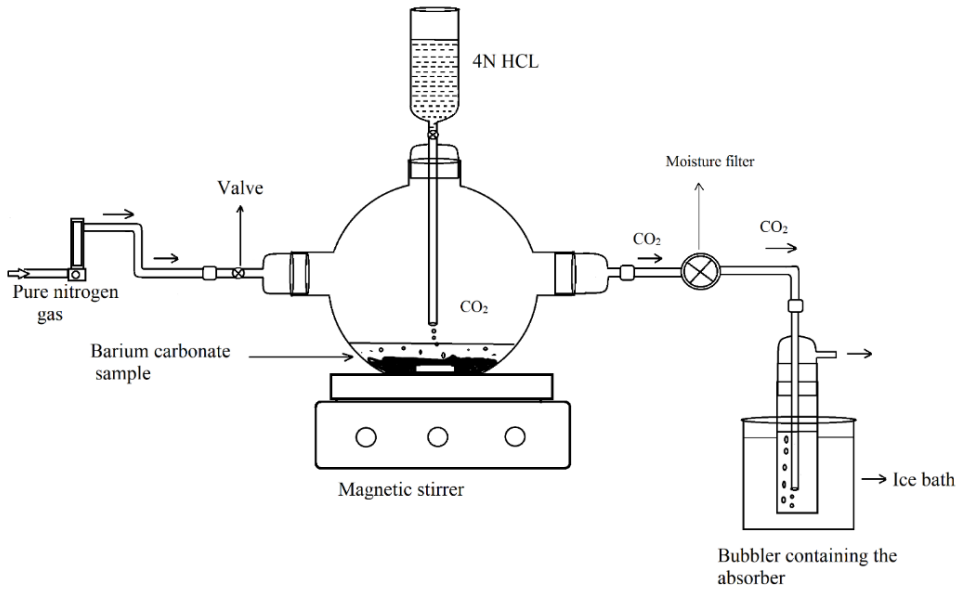

Fig. 2. Experimental setup for CO_2 regeneration from carbonate sample derived from ambient air and absorption in the absorber-scintillator mixture

In this way, an efficient regeneration and absorption of CO_2 were performed without any limitation on the weight of the carbonate sample. Upon saturation, the absorber-scintillator mixture was weighed again, and the mass of CO_2 absorbed was determined, transferred to low background polyethene LSC vial, shaken for

homogenization, sonicated, and stored in the dark for overnight so that the chemiluminescence is reduced before subjecting for liquid scintillation analysis.

4.2.5 Advantages of the new experimental setup

The improved method of CO_2 regeneration and absorption is advantageous when compared to the methods such as trapping the CO_2 in liquid nitrogen and the subsequent transfer through the airtight system under an inert atmosphere and closed-loop recirculation of gases, or the use of plastic bags or bladders reported previously (Molnár et al., 2006; Horvatinčić et al., 2004; Qureshi et al., 1989; Krajcar Bronić et al., 2009; Canducci et al., 2013; Varlam et al., 2007; Leaney et al., 1994) as it is simple and easy to use. A series of experiments were performed to ascertain the applicability of the improved CO_2 regeneration-absorption system. The time required to achieve saturation was about 35 - 40 min. This is a significant improvement over the previously reported time of 4 h (Joshi et al., 1987) and the overnight process reported by Baburajan et al. (2020); in both these cases, the absorber was not saturated with CO_2.

Experiments proved that, a highly reproducible result was obtained for each experiment with a high degree of saturation with a mean value of 2.1688 ± 0.075 g of CO_2/10 mL of the absorber. This highlight the advantages of the simple experimental arrangements developed in the present work.

4.3 Standardization of method for quantification of ^{14}C release through gaseous effluents

Two sample collection methodologies were adopted for this study: (i) Absorption of CO_2 by passing gaseous effluent through a set of gas washing bottles containing NaOH solution to trap CO_2; from now on, referred to as "conventional set-up", and (ii) an automated sampler to sample both oxide and reduced form of carbon.

4.3.1 Conventional set-up to sample only the oxidized form of ^{14}C

A gaseous effluent from the common stack-2 of Kaiga 3 & 4 was drawn through a set of three bubblers connected in series. The first bubbler with 100 mL of 1N HNO_3 was used to trap the tritium from the sampled gaseous effluents and the next two bubblers, each containing 100 mL of freshly prepared 2M ultra-pure NaOH solution (Merck reagent grade NaOH pellets), was for trapping oxide form of CO_2 species (Joshi et al., 1987, Olivier et al., 2005, Woo et al., 1999b, Molnar et al., 2006). The gaseous effluents samples were drawn from the sampling port of in the stack. The flow rate was adjusted for 1 L min^{-1}, and the sampling duration was 24 hours during weekdays and 48 hours during weekends. Care was taken to ensure that the flow rate remained constant throughout the sampling period. At the end of the sampling, the CO_2 absorbed NaOH solution from the two bubblers was collected in separate bottles, sealed to avoid contact with ambient air, and brought to the laboratory for analysis. The collection efficiency of the sampling set-up for CO_2 absorption was quantified to be ~ 82 % for a flow rate of 1 L min^{-1}, trap volume of 100 mL (the bubbler column diameter = 4.46 cm, which provides a NaOH trap height of 8 cm). However, the trapping efficiency of the bubbling system is not a crucial parameter for quantifying ^{14}C specific activity since it is determined based on the mass of CO_2 species taken for counting for liquid scintillation counting as given in equation 1 (Bharath et al., 2021).

4.3.2 Radiochemical analysis of the samples and determination of ^{14}C activity

In the laboratory, barium chloride solution ($BaCl_2$, 35 % w/v) was added in excess, and barium carbonate ($BaCO_3$) was precipitated from the NaOH. The precipitate was washed, dried, and ~ 2 g was taken for CO_2 regeneration and absorption in a specially designed CO_2 regeneration set-up (Bharath et al., 2021). Next, 4N

hydrochloric acid was added slowly to the carbonate sample to liberate CO_2. The produced CO_2 was trapped in an absorber-scintillator mixture of 10 mL of Carbosorb + 10 mL of PermaflourE+ (PerkinElmer, USA) through a bubbling process (Bharath et al., 2021). The mass of the CO_2 absorbed in the absorber-scintillator mixture was determined gravimetrically (accuracy of 0.1 mg), transferred to low background polyethylene liquid scintillation counting (LSC) vial, shaken for homogenisation, sonicated, and stored in the dark overnight to reduce chemiluminescence. It was then subjected to liquid scintillation counting (LSC) using Quantulus 1220 (PerkinElmer, USA) system. Data acquisition was performed using WINQ software (version 1.3), and spectrum processing was done with EASY VIEW software (version 1.2.0.16, PerkinElmer, USA). The optimised ^{14}C window used for the present study was 135-350 channels. Samples were measured in six intervals of 50 min, resulting in a total of 300 min per sample. From the mass of the CO_2 absorbed in the absorber and the counts obtained under the optimised counting window, the ^{14}C specific activity was calculated using equation (2) (Bharath et al., 2021).

4.3.3 Automated sampler for sampling both oxide and reduced forms of carbon

An automated air sampler (MRB-500, Mound Technical Solution, USA) was used to quantify both CO_2 and reduced form of release. The sample of gaseous effluents, drawn from the stack, was passed through a bubbler filled with 1N HNO_3 to trap tritium and then injected into a set-up of three glass vials of volume 20 ml in which the first two vials were filled with 15 mL of 1N NaOH solution. This set-up absorbs the CO_2 species from sampled gas. The third vial was empty and considered a safety vial to collect overflowing liquid from previous vials. The sampled gas from this vial set-up flows through a catalyst bed, maintained at 475 ^oC, to oxidize the reduced form into

CO_2. The oxidized gas was passed through another set-up of three vials, in which the first two vials were filled with 15 mL of 1N NaOH solution, and the third was empty. The flow rate was set at the maximum allowed value of 0.15 L min^{-1}, and the sampling duration was for a minimum of 50 h. After the sampling, the CO_2 absorbed NaOH sample was subjected to the same chemical treatment as explained in the previous section, and the activity was calculated using the equation (2).

Although the automated air sampler used in this study is capable of sampling both oxide and reduced forms of ^{14}C, we have used the conventional method, for sampling oxide forms of carbon since in this method, the flow rate and the volume of NaOH solution that can be used for sampling can be varied depending on the user requirements of long term and short term sampling routines. On the other hand, because of the very low flow rate and volume of the NaOH solution used for sampling in the automated sampler system, it is used for long term sampling programs. Moreover, the automated sampler was available for sampling only in the later stages of the study.

4.4 Ambient air sample collection in the vicinity of NPP and in the clean air region

The ambient air sampling campaign from the vicinity of Kaiga NPP was for two years. In December 2019, the samples were collected at three locations, and in October 2020, samples were collected from four locations. A map depicting the atmospheric air monitoring stations is shown in Fig. 1. The sampling procedure and processing remained the same as in section 4.3.1, the only difference being bubbler to trap tritium was not used. At each location, two sets of sampling were performed simultaneously. The sampling duration was 24 h at a flow rate of 2 L min^{-1}.

Ambient air samples were collected from the clean air region (region not affected by local anthropogenic sources of ^{14}C). In addition, several samples were collected at

the premises of the Centre for Advanced Research in Environmental Radioactivity (CARER), Mangalore University, about 20 km southeast of the coastal city of Mangalore. In the ambient air sampling, the total volume of air sampled was ~ 6 m^3 to obtain ~ 13 g of $BaCO_3$ (Bharath et al., 2021). The important difference between the ambient air ^{14}C activity measurement and that in gaseous effluents was the mass of the $BaCO_3$ taken for the regeneration of CO_2. In the case of gaseous effluents, ~ 2 g (accurately weighed) of $BaCO_3$ was taken, whereas it was ~ 13 g in the case of ambient air samples. This is because of the higher specific activity of ^{14}C of the gaseous effluents, and hence saturation of the absorber (Carbo-Sorb E) is not essential since the error associated with quench correction and background determination is negligible.

4.5 ^{14}C release in oxide form

The data from the automated sampling method were available for the year 2020 only, whereas, for the conventional method, it was for the period 2017 to 2020. In the year 2017 the normalized release rate varied in the range 0.12 - 0.55 TBq $GW(e)^{-1}$ a^{-1} with a GM of 0.20 TBq $GW(e)^{-1}$ a^{-1} (GSD = 1.75). Similarly the GM values for the years 2018, 2019 and 2020 were respectively 0.18 TBq $GW(e)^{-1}$ a^{-1} (GSD = 2.3), 0.02 TBq $GW(e)^{-1}$ a^{-1} (GSD = 2.0), 3.6 TBq $GW(e)^{-1}$ a^{-1} (GSD = 1.4). The GM value corresponding to the pooled data set of the four-year monitoring period was 0.27 TBq $GW(e)^{-1}$ a^{-1} (GSD = 8.1). The released rates were different for the different operating conditions (moderator cover gas purging and non-purging), which was as expected.

The reduced form of the ^{14}C release had a GM value of 49.8×10^{-3} TBq $GW(e)^{-1}$ a^{-1} (GSD = 1.3). The reduced form of ^{14}C release < 1.27 % (GM = 0.92 %) of the total release rate. Joshi et al. (1987) have reported this to be < 4 % for RAPS (2 PHWRs, each of 220 MW(e)), India. Kunz et al. (1974) have reported the reduced form in gaseous effluents of PWR to be > 80 %, whereas Schwibach et al. (1978) reported this

to be 43 % to 97 % for a PWR and less than 5 % for a BWR. Reviewing published reports worldwide, the IAEA (2004) has summarized that the reduced form of ^{14}C release from HWR varied from 2.5 % to 22 %.

4.6 ^{14}C activity in ambient air in the off-site locations of the NPP

The ambient air sampling campaign was during November – December 2019. The mean value of the excess activity was 48.3 Bq $kg^{-1}C$. A total of ten air samples were analysed from the clean air region, and the measured value of ^{14}C specific activity had a mean value and associated standard deviation of 229.0 ± 2.5 Bq $kg^{-1}C$ (101.3 ± 1.1 pMC). This matches well with the value of 226.7 Bq $kg^{-1}C$ (100.3 pMC) for the year 2019 for clean air data for the northern hemisphere (Levin and Kromer, 2004; Hammer et al., 2017). The maximum excess ^{14}C activity in the atmosphere, attributable to the release from the NPP, recorded for the 2019 sampling campaign was 65.1 Bq $kg^{-1}C$ with reference to the clean air region background activity of 229.0 Bq $kg^{-1}C$ for the corresponding year.

4.7 About Fluidyn Panach computer code

Fluidyn-PANACHE is a computer code dedicated to the 3-D simulation of the atmospheric processes related to the pollution and hazards in complex geometric environments and simulates the accidental dispersion from industrial sites. The basic equation used in Fluidyn-PANACHE is the Navier–Stokes equation. Species concentration, mass, and energy conservation equations are also solved. For turbulence models, PANACHE solves the Reynolds averaged forms of these equations. The governing equations are as follows:

(1) Conservation of species concentration

$$\frac{\partial \rho y_m}{\partial t} + \nabla.(\rho U y_m) = \nabla. D_m \nabla(y_m) + S_m \qquad m = 1,2.\ldots n$$

(4)

(2) Continuity equation

Formula (4) sums up all species and obtains a continuity equation (mass conservation)

$$\frac{\partial \rho}{\partial t} + \nabla(\rho U) = S_\rho \qquad (5)$$

(3) Navier–Stokes equation (conservation of momentum)

$$\frac{\partial(\rho U)}{\partial t} + \nabla.(\rho U U) = \nabla.\tau - \nabla p + S_U \qquad (6)$$

(4) Conservation of energy

$$C_p[\frac{\partial \rho T}{\partial t} + \nabla.(\rho U T)] = -\nabla.q + [\frac{\partial \rho}{\partial t} + U.\nabla\rho] + \tau : \quad \nabla U + S_T \qquad (7)$$

$$\tau = \mu\dot{\gamma}\left(\frac{2}{3}\mu - k\right)(\nabla.U)\delta \qquad (8)$$

$$\dot{\gamma} = \nabla U + (\nabla U)^T \qquad (9)$$

where τ is the viscous stress tensor; ρ is the density; γ is the rate of strain (rate of deformation) tensor; y_m is the mass fraction of species; U is the velocity vector; T is the temperature; p is the pressure; D_m is the effective diffusion coefficient of species; μ is the effective viscosity coefficient; κ is the expansion viscosity coefficient ($\kappa = 0$ is Stokes fluid); δ is the unit quantity; C_p is specific heat at constant pressure; q is the heat flux vector; $q = -k\Delta T$, k is the effective heat conduction coefficient; S_m represents the source term of the conservation equation of species m concentration; S_ρ represents the source term of the continuity equation; S_T is the source term of the conservation equation of energy; S_U represents the source term of the conservation equation of momentum.

Fluidyn-PANACHE uses modified standard k-ε turbulence model to resolve the turbulence structure within the domain. It includes a built-in automatic 3D mesh generator to create the computational finite-volume mesh around obstacles and body-

fitting the terrain undulations, which can be structured (rectangular) or unstructured (triangular). Clustering of mesh points in certain regions is possible with nested domains.

4.8 Boundary conditions

The equations (4-7) can be solved by assigning the boundary conditions for the main region, ground, and the obstacles. Boundary conditions characterize the profiles of model variables at outer domain boundaries and directly influence the simulated flow field and thus, the dispersion of the air pollutants. The top boundary of the domain was considered as an outflow boundary. The lateral boundaries, which depend on the wind direction with respect to the domain, based on wind direction, inflow and outflow boundaries are considered. The important input parameter for the dispersion study is wind velocity. In the atmosphere, wind does not flow at same velocity at different heights due to the frictional effect of the ground. The variation in the wind speed as a function of height in the surface boundary layer can be described by using power law.

4.9 CFD solver

The CFD tool Panache can solve nonlinear partial differential equations and solves in three dimensional space and time. It has MB and NT wind field solvers, MB solver is a pressure-based semi-implicit time-marching method on multi-block structured meshes. NT solver is a pressure-based fully implicit segregated method on unstructured meshes and it solves all governing equations separately. Panache can solve pollutant transport using two dispersion solvers, and they are standard and puff solvers. The standard dispersion solver solves a species mass conservation equation for each pollutant. Panache have several physical models such as air model, wind/temperature solution model, gravity model, turbulence model etc.

4.10 Performance evaluation of CFD model

The simulated results were evaluated against the measured results using standard statistical measures (Chang and Hanna, 2004), such as normalized mean square error (NMSE), fraction bias (FB), geometric mean bias (MG), geometric variance (VG), correlation coefficient (COR), factor of two (FAC2), and index of agreement (IA). These statistical measures characterize the agreement between the model prediction and the measured results. A perfect agreement between the modeled value and measured ones would have NMSE and FB=0, and COR, FAC2, MG, VG and IA=1 (Chang and Hanna, 2004). However, for an acceptable agreement between the simulated and measured values the criteria adopted one NMSE<4, -0.3<FB<0.3, FAC2>0.5, VG<1.3, 0.7<MG<1.3.

4.11 Validation of the CFD model:

The validation of the CFD model was performed by simulating a case for a flat terrain with no obstacles and for a steady state. The size of the computational domain was considered as 11000 m in length, 2000 m in width, and 250 m in height, which includes one point source (which represents the stack of the NPP) and the monitoring points at different distance from the point source in the central line of the plume (x-axis). A point source (stack) was defined at the left side of the domain with a height of 100 m. The release of pollutant ($^{14}CO_2$) from the source was simulated with a concentration of 1000 Bq m^{-3} (mass flux = 23.44 kg s^{-1}, exit velocity = 3.77 m s^{-1}). The wind condition was considered to be constant with a speed of 1 m s^{-1}, and the stability class D was considered. A 3-D unstructured mesh was selected, and the mesh was refined near the source and monitoring points. The simulation was performed to study

the plume dispersion and to predict the concentration at the desired point at the ground level.

The simulated results were validated with those obtained from the Gaussian plume model (GPM). The Gaussian model is one of the widely used dispersion model to calculate the concentration of a pollutant at a desired point under a steady state condition for flat terrain. In this model the concentration at ground level on the centre line of the plume was computed as under:

$$C_{(x,0,0)} = \frac{Q}{\pi \times U \times \sigma_y \times \sigma_z} \times e^{-\frac{H^2}{2\sigma_z^2}} \qquad 10$$

Where $C_{(x,0,0)}$ is the concentration at point x, ($C_{(x,y,z)} = C_{(x,0,0)}$, y & z are 0)

Q is the rate of emission of the pollutant from the source,

U is the prevailing wind speed,

H is the effective height of the plume central line,

σ_y and σ_z (m) are the standard deviations, which indicate the spread of the plume in the y and z directions, respectively,

The results obtained from GPM and the CFD simulation are compared in Fig 3. Statistical performance indicators were used to evaluate the agreement between the GPM and the simulated results of the model. The statistical analysis yielded NMSE=0.173, MG=1.19, FB=0.192, VG=1.157, FAC2=0.88. The NMSE value is smaller than it's acceptable bound (NMSE < 4), which shows that the predicted results have a relatively smaller scatter. The FB and MG values show that the simulated values have smaller under-prediction. The model predicts 88% of total concentration within a factor of two, which is in the acceptable range. This confirms that the CFD simulation is a very useful tool for predicting dispersion of the pollutants in the environment.

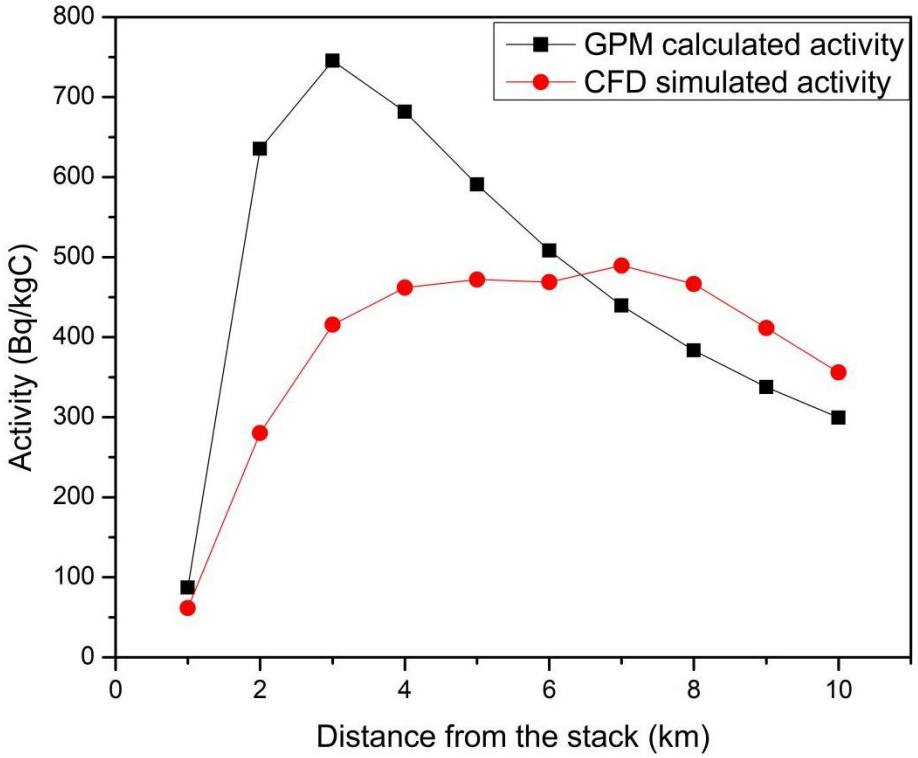

Fig. 3. Comparison between CFD simulated and GPM predicted 14C specific activity

4.12 Simulation of the dispersion of $^{14}CO_2$ released from the Kaiga NPP through gaseous effluents and experimental verification

After the validation of the model, simulations were performed by incorporating the topographical data of the Kaiga region to the CFD model. The terrain, pollutant, sources, and meteorological data were defined. The emission details such as mass flux, the concentration of pollutant species in the emission, exit velocity, and stack height have been aptly considered. The mesh is selected to be a 3-D unstructured mesh. A finer unstructured mesh is generated near the source, buildings. The domain is discretized into different vertical levels, the minimum vertical grid spacing is 1 m, and above certain height the spacing between the grid is increased. A steady-state simulation was carried out to establish the wind flow field and dispersion of $^{14}CO_2$ in the computational domain. Wind flow was solved by using NT-solver and for the dispersion standard solver was used. Appropriate physical models were used such as in-compressible air,

the temperature was in freeze and wind was solved. The buoyancy was selected as no gravity. Panache uses a modified standard k-ε turbulence model to resolve the turbulence structure within the domain. The k-ε turbulence model is the most validated and most widely applied model. This model is based on the Reynolds averaged Navier-Stokes (RANS) equations for CFD simulation.

The simulation was performed to predict the concentration at the atmospheric air monitoring points: monitoring station 1 situated at 2.3 km in the southwest direction, monitoring station and 2 situated at 4 km in the north direction from the Kaiga NPP. The ^{14}C specific activity was monitored at these two monitoring points. A total of seven simulations were performed, out of which four cases were for monitoring station 1, three cases for monitoring station 2.

The ^{14}C specific activity obtained from CFD simulation were compared with the experimental results and statistical analysis was performed. The statistical measures for the predicted and observed results were NMSE=2.86, FB=-0.38, MG=1.03, and FAC2=1.03. These values are all within the limits. The NMSE value showed that the scattering of the predicted results is small. The negative FB values indicate that an overall over-prediction of the simulated results. In general, the simulated results are in good agreement with the experimentally measured values of ^{14}C specific activity.

5. Outline of the Thesis

The thesis has been divided into six chapters. The contents of these chapters are briefly outlined below.

Chapter 1. Introduction and Literature Survey

This chapter presents the introduction and importance of the present study. It describes the origin, production rate, nuclear properties of ^{14}C behaviour in the environment and also the different mathematical models used for the atmospheric dispersion studies. A detailed review of the literature published in national and international journals on sources, existing methodologies for the measurements of ^{14}C and atmospheric dispersion models and solvers are presented in this chapter. Review reports published by International regulatory bodies, such as International Atomic Energy Agency (IAEA) and International commission for radiation protection (ICRP) are discussed in this chapter. The aim and objectives of the present study are also explained in detail in this chapter.

Chapter 2. Materials and Methods

The details of Kaiga NPP, geological and topographical feature of the Kaiga region are presented in this chapter. Details of the methodology incorporated for selection of sampling station, sample collection etc are explained. The chapter includes the details processing of the samples, and instruments. The CFD model, terrain details, pollutant, source, weather and mesh generation details are described in this chapter.

Chapter 3. Optimization studies

This chapter presents details of optimization of the method for determining ^{14}C activity in air samples, and optimization of parameters for ^{14}C measurement using LSC. Optimization of volume of air to be sampled, optimization of saturation characteristics of the absorber and mass of $BaCO_3$ required, development of a new CO_2 regeneration and absorption system for saturating the absorber, background, minimum detectable activity, and uncertainty, determination of counting efficiency are discussed here in detail.

Chapter 4. CFD simulation for the dispersion of $^{14}CO_2$ from the NPP

This chapter presents the atmospheric dispersion model used for the simulating the dispersion of the pollutant. Description of the Fluidyn-PANACHE computer code and numerical schemes, and boundary conditions used. Details of numerical simulations and statistical methods for performance evaluation are discussed in detail in this chapter.

Chapter 5. Results and discussion

This chapter presents the results and comprehensive discussion on the achievements of method optimization for the determination of ^{14}C specific activity by using liquid scintillation spectrometry method. The results and discussion can be broadly classified as following sections:

- ^{14}C release in oxide form, results of simultaneous measurements of oxide and reduced forms.
- Comparison of airborne ^{14}C release rate from Kaiga NPP with worldwide data
- ^{14}C specific activity in ambient air of clean air region and quantification of ^{14}C excess in the vicinity of NPP.
- Simulated data on ^{14}C specific activity in the monitoring points.
- Comparison of simulated results with experimental measurements.

All the data are analyzed rigorously through statistical tools to draw appropriate inferences and conclusions.

Chapter 6. Summary and Conclusions

The summary and conclusions drawn from the study are presented in this chapter. Some important findings and conclusions are as follows:

- A direct method with inexpensive and straight forward sample preparation system was tested for CO_2 absorption in the absorber and counting in a low background LSC for ^{14}C specific activity measurement in atmospheric air.
- The method is advantageous over the conventional methods (AMS and benzene conversion) for regular environmental monitoring programs as it is cost effective and involves simple sample preparation routine.
- A new experimental setup was developed, and optimized CO_2 absorption by the absorber and CO_2 loading up to ~ 2.3 g of CO2/10 mL with an average of 2.1688 g was achieved. The simplicity in the method and capability to achieve quick saturation of the absorber (< 45 min) is highly advantages in increasing the sample throughput, which is very important for the routine monitoring applications around the NPPs.
- A method for the ^{14}C release rate through the gaseous effluent from the stack was standardized, and both oxide and reduced forms of ^{14}C release was quantified for Kaiga NPP.
- The oxide and reduced forms of ^{14}C releases were quantified for the 4 × 220 MW(e) PHWR NPP at Kaiga, India. The GM value for the four-year monitoring data was 0.27 TBq $GW(e)^{-1}$ a^{-1} (GSD = 8.1).
- The reduced form of ^{14}C release had a GM value of 49.8×10^{-3} TBq $GW(e)^{-1}$ a^{-1} (GSD = 1.3). The relative percentage contribution of the reduced form of ^{14}C species was less than 1.27 % of the total release rate.
- A comparison between the normalized ^{14}C release rates of oxide form confirmed that release from the Kaiga NPP is similar to those reported for other PHWR NPPs.

- The measured mean of the release rate (1.08 ± 1.80 TBq $GW(e)^{-1}$ a^{-1}) was in agreement with the calculated value (0.94 TBq $GW(e)^{-1}$ a^{-1}), based on the design of the 220 MW(e) Indian PHWR.
- The measured value of excess ^{14}C activity in ambient air at different monitoring stations in the off-site areas of the Kaiga NPP due to the stack release depends upon the prevailing wind regime. Sampling locations on the axis of the downwind direction exhibit higher excess ^{14}C activity.
- The release rate calculated based on the excess ^{14}C specific activity in the ambient air in different air monitoring stations in the vicinity of the NPP and the established dilution factor corresponding to the sampling station agreed with the measured values within a factor ~ 3.
- Applicability of the CFD model Fluidyn-PANACHE computer code used to performe a 3-D CFD simulations for plume dispersion in a complex environment was examined.
- The wind flow and dispersion of $^{14}CO_2$ was simulated, concentration was plotted at the monitoring points. Statistical evaluation confirmed that simulated result was similar to the measured values confirming that the CFD model Fluidyn-PANACHE can be used for the dispersion of the pollutant in a complex terrain for emergency response planning and management.

6. Research Publications in Peer-Reviewed Journals, National and International Conferences Related to the Thesis Work

a. Journal Publications

1. **Bharath, S**., Arya Krishnan, K., Renita Shiny D'Souza., Rashmi Nayak, S., P.M. Ravi, Rajveer Sharma, Pankaj Kumar, Sundeep Chopra, N. Karunakara, 2021.

Optimisation of CO_2 absorption and liquid scintillation counting method for carbon-14 specific activity measurement in atmospheric air. Appl. Radiat. Isot. 172.

2. **Bharath**, K. Arya Krishnan, Renita Shiny D'Souza, S. Rashmi Nayak, B.N. Dileep, P.M. Ravi, S.S. Mangavi, G.S. Salunke, D. Veerendra, N. Karunakara, 2022. Carbon-14 emission from the pressurized heavy water reactor nuclear power plant at Kaiga, India. J. Environ. Radioact. 225

3. **Bharath**, Venkatesan R, Veerendra D, Karunakara, 2024. Computational fluid dynamics (CFD) based simulation and experimental validation of dispersion of $^{14}CO_2$ released from the gaseous effluent stack of a nuclear power plant situated in a complex terrain. Sci. Total Environ. (communicated)

b. International Conferences

1. **Bharath**, R.S. D'Souza, S.R. Nayak, Dileep B. N., S.S. Manganvi, Ravi P. M., Karunakara N, 2019. An improvised method for Carbon-14 measurement in gaseous effluents. 5th International Conference on Environmental Radioactivity (ENVIRA 2019), 8–13 September 2019, Praha, Czech Republic, https://doi.org/10.14311/ENVIRA.2019.

2. **Bharath**, Arya Krishnan K, Renita Shiny, Rashmi Nayak, Dileep N. B, Ravi M. P, Karunakara N, 2022. Carbon-14 specific activity in atmospheric air in the vicinity of a PHWR nuclear power plant in India. 6th European Congress on Radiation Protection, 30 May – 3 June 2022, Budapest, Hungary.

3. **Bharath**, Arya Krishnan K, Manganvi S. S, Veerendra D, G. S. Salunke, Karunakara N, 2022. Comparison of airborne 14C release rate from Kaiga NPP with other NPPs of the world. 6th Asian and Oceanic Congress for Radiation Protection (AOCRP6), 07-11, February 2023, Nehru centre, Worli, Mumbai.

c. National Conferences

1. **Bharath**, Arya Krishnan, N Karunakara, 2022. Carbon-14 dose in the environment from the natural sources. 2nd National Conference on Radiation Physics (NCRP-2022), 15-16 December, 2022, Bangalore University, Bangalore.
2. **Bharath**, Arya Krishnan, S.S. Mangavi, D. Veerendra, G.S. Salunke, N Karunakara, 2023. Quantification of oxide and reduced forms of 14C release from the Kaiga NPP. 23rd National Symposium on Radiation Physics (NSRP), 19-21, January 2023, University of Mysore, Mysuru.

Place: Mangalagangothri — Bharath
Date: — Research Student

Place: Mangalagangothri — Karunakara N
Date: — Research guide

References

Baburajan, A., Dalvi, S.S., Sudheendran, V., Varakhedkar, V.K., Saradhi, I.V., Ravi, P.M., Karunakara, N., 2020. Validation of a method for measurement of 14C in air and its application for estimation of 14C levels around Tarapur nuclear site. J. Radioanal. Nucl. Chem. 324, 551–559.

Bharath, K. Arya Krishnan, Renita Shiny D'Souza, S. Rashmi Nayak, B.N. Dileep, P.M. Ravi, S.S. Mangavi, G.S. Salunke, D. Veerendra, N. Karunakara, 2022. Carbon-14 emission from the pressurized heavy water reactor nuclear power plant at Kaiga, India. J. Environ. Radioact. 225

Bharath, S., Arya Krishnan, K., Renita Shiny D'Souza., Rashmi Nayak, S., P.M. Ravi, Rajveer Sharma, Pankaj Kumar, Sundeep Chopra, N. Karunakara, 2021. Optimisation of CO_2 absorption and liquid scintillation counting method for carbon-14 specific activity measurement in atmospheric air. Appl. Radiat. Isot. 172.

Canducci, C., Bartolomei, P., Magnani, G., Rizzo, A., Piccoli, A., Tositti, L., Esposito, M., 2013. Upgrade of the CO_2 direct absorption method for low level ^{14}C liquid scintillation counting. Radiocarbon 55 (2 - 3), 260–267.

Chang, J.C., Hanna, S.R., 2004. Air quality model performance evaluation. Meteorol. Atmos. Phys. 87 (1-3), 167-196. http://dx.doi.org/10.1007/s00703-003-0070- 7.

D'Souza, R.S., Nayak, R.S., Mohan, M.P., Bharath, S., Arya Krishnan, K., Kamath, S., Di´eguez, A., Agullo, L., Gomez Martínez, I., Santos-Ar´evalo, F.J., García-Tenorio, R., Ravi, P.M., Karunakara, N., 2020. Optimisation of a batch thermal combustion method using a tube furnace oxidation system (pyrolyser) and LSC for carbon-14 determination in environmental matrices. J. Environ. Radioact. 226 https://doi.org/ 10.1016/j.jenvrad.2020.106345

D'Souza, R.S., Nayak, R.S., Mohan, M.P., Bharath, S., Arya Krishnan, K., Kamath, S., Di´eguez, A., Agullo, ´ L., Gomez ´ Martínez, I., Santos-Ar´evalo, F.J., García-Tenorio, R., Ravi, P.M., Karunakara, N., 2020. Optimisation of a batch thermal combustion method using a tube furnace oxidation system (pyrolyser) and LSC for carbon-14 determination in environmental matrices. J. Environ. Radioact. 226 https://doi.org/ 10.1016/j.jenvrad.2020.106345

Dias, C.M., Telles, E.C., Santos, R.V., Stenstrom, ¨ K., Nícoli, I.G., Correa, R.S., Skog, G., 2009. 14C, $\delta^{13}C$ and total C content in soil around a Brazilian PWR power plant. J. Environ. Radioact. 100, 348–353.

D'Souza, R.S., Nayak, R.S., Bharath, S., Mohan, M.P., Dileep, B.N., Ravi, P.M., Karunakara, N., 2019. Importance of site-specific data on carbon content in environmental matrices for accurate determination of carbon-14 specific activity. J. Radioanal. Nucl. Chem.

Godwin, H., 1962. Half-life of radiocarbon. Nature. 195:984.

Hammer, S., Friedrich, R., Kromer, B., Cherkinsky, A., Lehman, S., Meijer, H., Uchida, M., 2017. Compatibility of Atmospheric $^{14}CO_2$ Measurements: Comparing the Heidelberg Low-Level Counting Facility to International Accelerator Mass Spectrometry (AMS) Laboratories. Radiocarbon, 59(3), 875-883. doi:10.1017/RDC.2016.62

Hill, R., Arnott, A., Hayden, P., Lawton, T., Robins, A., Parker, T., 2011. Evaluation of CFD model predictions of local dispersion from an area source on a complex industrial site. Int. J. Environ. Pollut. 44, 173e181.

Horvatinˇci´c, N., Bareˇsi´c, J., Karjcar Broni´c, I., Obeli´c, B., 2004. Measurement of low ^{14}C activities in a liquid scintillation counter in the Zagreb radiocarbon laboratory. Radiocarbon 46 (1), 105–116. https://doi.org/10.1017/s0033822200039412.

Hsieh, K.-J., Lien, F.-S., Yee, E., 2013. Dense gas dispersion modeling of CO2 released from carbon capture and storage infrastructure into a complex environment. Int. J. Greenh. Gas Control 17, 127e139

International Atomic Energy Agency (IAEA), 1989. IAEA/RCA. Measurement of radionuclides in food and environment. Technical report series. 295. IAEA, Vienna.

International Atomic Energy Agency (IAEA), 2004. Management of waste containing tritium and carbon-14. Report IAEA 421, Vienna.

Josh, M.L., Ramamirtham, B., Soman, S.D., 1987. Measurement of ^{14}C emission rates from a pressurized heavy water reactor. Health Phys. (52): 787-791.

Kamath, S., Narayana, B., D'Souza, R.S., Nayak, R.S., Mohan, M.P., Dileep, B.N., Baburajan, A., Ravi, P.M., Karunakara, N., 2019. Tritium in water bodies around Kaiga generating station, J. Radioanal. Nucl. Chem. 322, 389-397.

Karlén, I., Olsson, 1.U., Kållberg, P., Kilicci, S., 1964. Absolute determination of the activity of two ^{14}C dating standards. Ark. Geofys. 4: 465-477.

Karunakara, N., Avadhani, D.N., Mahesh, H.M., Somashekarappa, H.M., Narayana, Y., Siddappa, K., 2000. Distribution an environment of ^{210}Po in the environment of Kaiga in South India, J. Environ. Radioact. 51, 349-362.

Karunakara, N., Avadhani, D.N., Mahesh, H.M., Somashekarappa, H.M., Narayana, Y., Siddappa, K., 2001. ^{137}Cs concentration in the environment of Kaiga in the southwest coast of India, Health Phys. 81, 148-155.

Karunakara, N., Chetan Rao, Ujwal, P., Yashodhara, I., Kumara, S., Ravi, P.M. 2013a. Soil to rice transfer factors for ^{226}Ra, ^{228}Ra, ^{210}Pb, ^{40}K and ^{137}Cs: a study on rice grown in India. J. Environ. Radioact. 118, 80-92. Doi:10.1016/j.jenvrad.2012.11.002

Karunakara, N., Ujwal, P., Yashodhara, I., Chetan, Rao, Sudeep Kumara, K., Dileep, B. N., Ravi, P. M. 2013b. Studies on soil to grass transfer factor (Fv) and grass to milk transfer coefficient (Fm) for cesium in Kaiga region. J. Environ. Radioact. 124, 101-112. https://doi.org/10.1016/j.jenvrad.2013.03.008.

Krajcar Broni´c, I., Horvatinci´c, N., Baresi´c, J., Obeli´c, B., 2009. Measurement of 14C activity by liquid scintillation counting. Appl. Radiat. Isot. 67 (5), 800–804.

KrajcarBronić, I., Barešić, J., Sironić, A., Borković, D., 2020. Properties, behaviour and potential health effects of ^{14}C. In: Radionuclides, Nova Science Publishers, Inc. ISBN: 978-1-53617-379-6.

Kunz C., Mahoney W. E. and Miller T. W., 1974, "Carbon- 14 gaseous effluent from pressurized water reactors," Paper presented at Health Physics Society Symp. On population exposures, Conf-741018 (Oak Ridge, TN: Office of Scientific and Technical Information).

Leaney, F.W., Herczeg, A.L., Dighton, J.C., 1994. New developments for the direct CO_2 absorption method for radiocarbon analysis. Quat. Sci. Rev. 13 (2), 171–178.

Levin, I., Kromer, B., 2004. The Tropospheric $^{14}CO_2$ Level in Mid-Latitudes of the Northern Hemisphere (1959–2003). Radiocarbon, 46(3), 1261-1272. doi:10.1017/S003382220 0033130

Levin, I., Kromer, B., Schoch-Fischer, H., Bruns, M.,Munnich, M., Berdau, B., Vogel, J. C., Munnich, K.O., 1985. 25 years of tropospheric ^{14}C observations in Central Europe. Radiocarbon. 27(1):1-19.

Libby, W.F., 1946. Atmospheric helium three and radiocarbon from cosmic radiation. Phys. Rev. 69, 671–672.

Libby, W.F., 1965. Radiocarbon Dating (2nd (1955)ed.). Chicago: Phoenix.

Mazeika, J., Petrosius, R., Pukiene, R., 2008. Carbon-14 in tree rings and other terrestrial samples in the vicinity of Ignalina Nuclear Power Plant, Lithuania. J. Environ. Radioact. 99, 238–247. https://doi.org/10.1016/J.JENV RAD .2007.07.011.

Mazzoldi, A., Hill, T., Colls, J.J., 2008. CFD and gaussian atmospheric dispersion models: a comparison for leak from carbon dioxide transportation and storage

facilities. Atmos. Environ. 42 (34), 8046e8054. http://www.sciencedirect.com/science/article/pii/S1352231008006080.

Mazzoldi, A., Hill, T., Colls, J.J., 2011. Assessing the risk for CO2 transportation within CCS projects, CFD modelling. Int. J. Greenh. Gas Control 5, 816e825.

Molnar, M., Nagy, S., Svingor, E., Svetlik, I., 2006. Refining the CO_2 absorption method for low-level ^{14}C liquid scintillation counting in the ATOMKI. In: Chalupnik S, Schonhofer F, NoakesJE, editors. LSC 2005: Advances in liquid scintillation spectrometry. Tucson: Radiocarbon. 407-415.

Nair, A.R., Sinha, U.K., Joseph, T.B., Rao, S.M., 1995. Radiocarbon dating up to 37,000 years using CO_2 absorption technique. Nucl. Geophys. 9 (3), 263–268.

Nayak R.S., Renita S.D., Srinivas K.S., Mohan M.P., Bharath S., Trilochana S., Sudeep K., Narayana B., Dileep B.N., Ravi P.M., Karunakara N., 2019. Organically bound tritium: optimization of measurements in environmental matrices by combustion method and liquid scintillation spectrometry. J. Radioanal. Nucl. Chem. 319, 917–926.

Noakes, J., Norton, G., Culp, R., Nigam, M., Dvoracek, D., 2006. A comparison of analytical methods for the certification of biobased products. In: Chalupnik, S., Schonhofer, ¨ F., Noakes, J.E. (Eds.), LSC 2005: Advances in Liquid Scintillation Spectrometry. Radiocarbon, Tucson, pp. 259–271.

Norton, G.A., Devlin, S.L., 2006. Determining the modern carbon content of biobased products using radiocarbon analysis. Biosource Technol 97 (16), 2084–2090.

Olivier, A., Tenailleau, L., Baron, Y., Maro, D., Fontugne, M., 2005. Measurement of the carbon-14 activity at natural level in air samples. J. Radioprotection. Vol 40, 791-796.

Otlet, R.L., Walker, A.J., Fulker, M.J., Collins, C., 1997. Background carbon-14 levels in UK foodstuffs, 1981 - 1995, based upon a 1992 survey. J. Environ. Radioact. 34, 91–101.

Popoaca, S., Bucur, C., Simionov, V., 2014. Determination of ^{3}H and ^{14}C in organic sample after separation through combustion method. J. Energ. Eng. 8, 1687-1694.

Povinec, P.P., Šivo, A., Ješkovský, M., Svetlik, I., Richtáriková, M., Kaizer, J. 2015. Radiocarbon in the atmosphere of the Žlkovce monitoring station of the Bohunice NPP: 25 years of continuous monthly measurement, Radiocarbon, 57(3)1–8. DOI:10.2458/azu_rc.57.18364.

Qureshi, R.M., Aravena, R., Fritz, P., Drimmie, R., 1989. The CO2 absorption method as an alternative to benzene synthesis method for LSC dating. Appl. Geochem. 4 (6), 625–633.

Qureshi, R.M., Aravena, R., Fritz, P., Drimmie, R., 1989. The CO_2 absorption method as an alternative to benzene synthesis method for LSC dating. Appl. Geochem. 4 (6), 625–633.

Roussel-Debet, S., Gontier, G., Siclet, F., Fournier, M., 2006. Distribution of carbon 14 in the terrestrial environment close to French nuclear power plant. J. Environ. Radioact. 87, 246–259.

Schwibach J., Riedel H. and Bretschneider J., 1978. Investigations into the Emission of Carbon-14 Compounds from Nuclear Facilities, Commission of the European Communities, Health and Safety Directorate, Jean Monnet Building, Luxembourg, Report no. V-3062/78-EN.

Sharma, P.K., B. Gera and A.K. Ghosh., 2011. Comparison of atmospheric dispersion in a large terrain of Kaiga Atomic Power Plant with simple terrain assumption

against actual complex terrain modelling. International Journal of Environmental Sciences, Vol. 1.

Singleton, D.L., Sanchez, A.L., Woods, C., 2002. A comparison of two techniques to determine carbon-14 in environmental samples. J. Radioanal. Nucl. Chem. 251 (3), 353–357.

Sohn, W., Kang, D. W., Kim, W. S., 2004. An estimate of carbon-14 inventory at Wolsong nuclear power plant in the Republic of Korea, J. Nucl. Sci. Technol., 40, 604–613.

Stenström, K. E., Skog. G., Elisavet. G., Genberg, Johansson, A., 2011. A guide to radiocarbon unitsand calculations. Internal Report LUNFD6(NFFR-3111)/1 - 17/(2011). Lund University, Department of Physics, Division of Nuclear Physics, Sweden.

Stenström, K., Erlandsson, B., Mattsson, S., Thornberg, C., Hellborg, R., Kiisk, M., Persson, P., Skog, G., 2000. ^{14}C emission from Swedish nuclear power plants and its effect on the ^{14}C levels in the environment. (Report 06/00 LUNDFD6/(NFFR-3079)/1-44/(2000) Lund 2000).

Stenstrom,K., 1995. New Applications of ^{14}C Measurements at the Lund AMS Facility. Doctoral dissertation. Lund University, Sweden.

United Nations Scientific Committee on the effect of atomic radiation (UNSCEAR), 1977. Sources and effects of Ionizing radiation, United Nations, New York.

United Nations Scientific Committee on the Effects of Atomic Radiation (UNSCEAR), 2017. Sources, Effects and Risks of Ionizing Radiation. United Nations Scientific Committee on the Effects of Atomic Radiation, UNSCEAR 2016

Report to the General Assembly with Scientific Annexes, United Nations, New York.

United Nations Scientific Committee on the Effects of Atomic Radiation (UNSCEAR), 2010. Sources and Effects of Ionizing Radiation. Volume I: Sources: Report to the General Assembly, Scientific Annexes A and B. UNSCEAR 2008 Report. United Nations Scientific Committee on the Effects of Atomic Radiation. United Nations, New York.

United Nations Scientific Committee on the Effects of Atomic Radiation (UNSCEAR), 2000. Sources (Volume 1), Effects (volume II). United Nations, New York.

United Nations Scientific Committee on the Effects of Atomic Radiation (UNSCEAR), 1993. Sources and effects of ionizing radiation, Report to the General Assembly with scientific annexes. United Nations Scientific Committee on the Effects of Atomic Radiation, New York.

Vagner, I., Varlam, C., Faurescu, D., Bogdan, D., Faurescu, I., 2019. Reproducibility of CO_2 absorption method for measurement of radiocarbon using a PARR bomb and LSC. Radiocarbon 61, 1835–1842. https://doi.org/10.1017/rdc.2019.94.

Varlam, C., Stefanescu, I., Varlam, M., Popescu, I., Faurescu, I., 2007. Applying the direct absorption method and LSC for ^{14}C concentration measurement in aqueous samples. Radiocarbon 49 (2), 281–289.

Woo, H.J., Cho, S.Y., Chun, S.K., Kim, N.B., Kang, D.W., Kim, E.H., 1999b. Optimisation of liquid scintillation counting techniques for the determination of Carbon-14 in environmental samples. J. Radioanal. Nucl. Chem. 239(3), 649-655.

Woo, H.J., Cho, S.Y., Chun, S.K., Kim, N.B., Kang, D.W., Kim, E.H., 1999a. Sample treatment techniques for the determination of environmental radiocarbon in a nuclear power station area. J. Radioanal. Nucl. Chem. 239 (3), 533–538.

Xing, J., Liu, Z., Huang, P., Feng, C., Zhou, Y., Zhang, D., Wang, F., 2013. Experimental and numerical study of the dispersion of carbon dioxide plume. J. Hazard. Mater. 256-257, 40-48.